Geomagnetically Induced Currents, Transformer Harmonics, and Reactive Power Impacts of the Gannon Storm in May 2024

M. A. Clilverd[1], C. J. Rodger[2], D. H. Mac Manus[2], J. B. Brundell[2], M. Dalzell[3], A. Renton[3], Victor Lo[3], A. Lapthorn[4], Andrew W. Smith[5], John Malone-Leigh[2], Xinhu Feng[2], and Tanja Petersen[6]

[1]British Antarctic Survey (UKRI- NERC), Cambridge, United Kingdom.

[2]Department of Physics, University of Otago, Dunedin, New Zealand.

[3]Transpower New Zealand Limited, Wellington, New Zealand.

[4]Department of Electrical and Computer Engineering, University of Canterbury, Christchurch, New Zealand.

[5]Department of Mathematics, Physics and Electrical Engineering, University of Northumbria, Newcastle upon Tyne, United Kingdom.

[6]Department of Data Science and Geohazards Monitoring, GNS Science, Lower Hutt, New Zealand.

Corresponding author: Mark Clilverd (macl@bas.ac.uk)

Key Points:

- Geomagnetically induced current (GIC) measurements were analyzed for two high voltage transformers during the May 2024 Gannon Storm.
- Linear enhancements of even order AC harmonics occurred at GIC >30 A, consistent with asymmetric half-cycle transformer core saturation.
- Reactive power consumption responses to GIC are determined for a commonly used transformer type: 3 phase, 3 limb, wye-grounded, 220 kV.

Abstract

Geomagnetically induced current (GIC) measurements made at two 3 phase, 3 limb transformers, operating in the Halfway Bush substation in Dunedin, New Zealand have been analyzed during the May 2024 Gannon Storm. GIC measurements were combined with very low frequency radio wave AC harmonic measurements made nearby, and reactive power measurements made at key points in the substation. This study focuses on the 11 May, 00 -14 UT period when geomagnetic activity was high and the 220 kV transformers, T6 and T3, experienced multiple short periods where GIC > 50 A in each transformer, maximizing at 113 A. During high GIC periods linear enhancements of even order AC harmonic intensity were identified, particularly for the 2nd and 4th harmonics, consistent with asymmetric half-cycle transformer core saturation. Reactive power consumption (Q_{con}, MVAr) increased linearly when GIC levels were >30 A, consistent with the enhancement of even order AC harmonics due to transformer core saturation >30 A DC. Transformer T6 exhibited a reactive power response of 0.038 MVAr/A, while for T3 it was 0.026 MVAr/A. Simple extrapolation of these findings to extreme storm modelling of the New Zealand high voltage grid suggests that an additional ~200-350 MVAr of generation would be required to compensate for peak increased reactive power consumption at 19 of the most affected sites during a Carrington-level event. Such additional power requirements are likely to be within the capabilities of the power generation network.

Plain Language Summary

During large geomagnetic storms high levels of quasi DC currents can be induced in long, low resistance, high voltage power lines. The currents flow to ground through substation transformers that are grounded at each end of the line on the high voltage side when they complete an electrical circuit that uses the ground as a return path, i.e., not all transformers. High DC or quasi DC current levels can cause transformers to operate outside of their design parameters. Such conditions can cause internal heating, tripping, and potentially failure of the transformer. A sign of a transformer under stress from induced DC is the generation of even order AC harmonics through asymmetric half-cycle transformer core saturation. Another response is increased consumption of reactive power by the transformer. These conditions occurred during the May 2024 Gannon geomagnetic storm at Transpower’s Halfway Bush substation in Dunedin, New Zealand. Even order AC harmonic intensity was observed to increase with increasing DC levels, as well as increased reactive power consumption. Such measurements of the response of transformers to induced DC are rare. The results presented here provide key understanding of the response of a commonly used transformer type to geomagnetically induced currents.

1 Introduction

Large geomagnetic storms are a space weather hazard to power transmission networks due to the effects of Geomagnetically Induced Currents (GICs). Disturbances of the Earth's external magnetic field Birkeland, 1908; Oughton et al., 2017) induce geo-electric fields within the conducting surface of the Earth, and drive electric currents in power transmission lines (Vasseur and Weidelt, 1977; Beggan et al., 2013; Divett et al., 2017; 2020). GIC flowing in power lines can pass to ground through the neutral-ground connections of transformers (Mac Manus et al., 2022). GIC can negatively impact power transmission systems through asymmetric half-cycle transformer core saturation (Arrillaga and Watson, 2003; Rodger et al., 2020). Effects on transformers are expected to result in increased reactive power losses, waveform distortion, and heating due to stray fields (Samuelsson, 2013; Boteler, 2015).

The generation of even-order current and voltage harmonics of the power transmission frequency (typically 50 or 60 Hz) are a sign of a transformer operating outside of its design range. The presence of even harmonics can be used as an indicator of asymmetric saturation due to GIC (Boteler et al., 1989; Rodger et al., 2020). GIC potentially leads to damaging levels of internal heating, voltage dips, power flow variations, and distortion of the AC supply waveform. Reactive power losses within transformers can lead to increased system loading and could result in voltage collapse if the increased load required exceeds the capability of the network. The propagation of harmonic distortion power away from its transformer source (e.g., Crack et al., 2024) can also cause networks to become destabilized through the incorrect operation of protective relays, affecting the capability of the network to provide the additional load required by reactive power losses. Such even-order harmonics contributed to the blackout of the Québec power system in March 1989 through the inappropriate operation of protective relays (Béland and Small, 2004; Guillon et al., 2016). As such, the presence of even-order harmonics can be a sign of transformers under stress, with reactive power responses and internal heating expected at the same time (Rajput et al. 2020).

In New Zealand the high voltage power transmission network, operated by Transpower New Zealand Ltd, has been equipped with >70 LEM neutral current monitors, the number of instruments gradually increasing since 2001. The DC measurements are located on key transformers and can be used to determine the levels of GIC (Mac Manus et al., 2017; Rodger et al., 2020). Transformers located in the South Island city of Dunedin have been shown to experience comparatively high GIC levels during geomagnetic storms (Rodger et al., 2017; Mac Manus et al., 2022). As result of this, wideband very low frequency (VLF) measurements have been undertaken by a radiowave receiver located close to the Halfway Bush (HWB) substation in Dunedin since 2016. This experimental setup was described in detail in Clilverd et al. (2018). The VLF instrument detected even-order harmonics generated by a single phase bank transformer (T4) experiencing 45 A of GIC during a large geomagnetic storm in September 2017 (Clilverd et al., 2018; Rodger et al., 2020). However, after the removal of the single phase transformer T4 in November 2017 the observation of even-order harmonics at HWB appeared to become much less likely as the remaining three phase, three limb units appear to be less responsive to GIC (e.g., Price, 2002; Mac Manus et al., 2022). Subsequent moderate geomagnetic storms have confirmed this, with lower harmonic levels observed for moderate geomagnetic storms following the decommissioning of HWB T4 (Clilverd et al., 2020; Crack et al., 2024).

One key question regarding three phase transformers concerns the GIC level at which half-cycle saturation occurs. The threshold for increased reactive current draw is a function of the saturation curve of the transformer, and some transformers have more or less headroom before they start to enter saturation. Mac Manus et al. (2022) investigated the impact of mean current danger levels for three phase, three limb transformer units starting from 200 A, based on a transformer design modelling study commissioned by Transpower. Rezaei-Zare et al. (2016) modelled the three phase, three limb 125 MVA, 230 kV transformer response to GIC, concluding that there was a neutral GIC threshold below which no appreciable reactive power response occurred. However, the simulations showed that above the GIC threshold the saturated core leads to increasing reactive power consumption. The threshold levels modeled were sensitive to the design of the transformer (such as the AC excitation level), and tests showed reactive power responses starting for neutral GIC ranging over 25-100 A. Detailed transformer modeling results with varying design features predicted reactive power consumption responses of 0.08 to 0.16 MVAr/A once the neutral current threshold was exceeded. However, Dong et al. (2001) presented transformer saturation test results and simulations for 3 phase, 3 limb transformers that showed no GIC threshold, i.e., a threshold close to 0 A, and reactive power consumption responses of 0.29 MVAr/A. Additionally, simulations undertaken by Dong et al. suggested that the 3 phase, 3 limb design would exhibit 3 different MVAr/A gradients, k1, k2, k3 – each with a lower gradient than the previous one - each with increasing GIC thresholds. Dong et al. (2001) tabulated test results up to 120 A (per transformer) which showed no change of gradient from the initial k1 level (0.29 MVAr/A). Bonmann et al. (2024) described the results of injecting 0 -200 A DC currents into a 3 phase, 3 limb 1000 MVA autotransformer connected to a 420 kV bus. Linear increases in reactive power began at DC currents >50 A, with a response of 0.17 MVAr/A. A 3 phase, 5 limb transformer showed reactive power responses at ~5 A and above, showing how important transformer design is to any GIC response.

The recent geomagnetic storm of 10-11 May 2024, identified here as the Gannon storm in honor of Jennifer L. Gannon (1978-2024), produced large geomagnetic storm signatures (Kp=9, G5). Starting at ~17:00 UT on 10 May 2024, large magnetic field perturbations were observed around the world for approximately 24 hours. In New Zealand the largest perturbations of the geomagnetic field occurred during 11 May 2024. Just before 00:00 UT on 11 May 2024 Transpower enacted the NZ-wide GIC mitigation plan based on the one described in Mac Manus et al. (2023) as TP2022NZ. In this mitigation plan 24 line disconnections, and the disconnection of the series winding of 1 transformer are undertaken. The timing of network changes are particularly important for our study as HWB is a known hot spot for GIC (Mac Manus et al., 2022, Smith et al., 2024) and the mitigation changes are partly focused on the Dunedin section of the network. Prior to this, in the initial storm period from 17:00 UT to 24:00 UT on 10 May 2024, some protective changes to the network configuration were made, particularly in the South Island. In Dunedin, additional network changes occurred when transformer number T2 in the South Dunedin substation went offline at about 17:28 UT

(Transpower, 2024), although the tripping of T2 was not thought to be directly due to Gannon storm.

In this study we combine GIC measurements made at two transformers in the Halfway Bush substation in Dunedin with VLF harmonic measurements made nearby, and reactive power measurements, *Q*, made at key points in the substation. Local magnetic field variations were determined from the Swampy Summit magnetometer, located a few km outside of Dunedin. Detailed analysis of the impact of GIC on the Halfway Bush substation transformers is undertaken for 11 May 2024, i.e., after the GIC mitigation plan had been enacted and the network conditions remained relatively constant. Section 2 describes the local magnetic field perturbations that induced elevated GIC in the Dunedin region, and the Halfway Bush substation layout during the storm. Section 3 investigates the harmonic distortion responses to the GIC events and considers the threshold for which some level of transformer half cycle saturation was observed. Section 4 identifies reactive power responses to high levels of GIC, determining the relationship between the applied current and reactive power consumption, Q_{con}, for the three phase, three limb transformers located at the HWB substation. Discussion and Conclusions are presented in sections 5 and 6.

2 Geomagnetic conditions and the Halfway Bush substation configuration on 11 May 2024

The response of the transformers in the HWB substation, Dunedin, New Zealand, is dependent on the local magnetic field variations, as well as the nature and number of GIC-impacted transformers in the substation. Figure 1 shows the rate of change of the horizontal magnetic field strength, *H*, where *H* is calculated in the usual way using the north magnetic field component *X*, and the east component *Y*, i.e., $H=\sqrt{(Y^2+X^2)}$. Magnetic field variations were measured at New Zealand's official magnetic observatory, Eyrewell near Christchurch, and also at the Swampy summit site close to Dunedin (Rodger et al., 2017; Clilverd et al., 2018). These magnetometers are separated by ~300 km, with Eyrewell being at lower geomagnetic latitude than Swampy Summit. The upper panel shows Eyrewell d*H*/d*t* for 11 May 2024, with the original 1 s data mean averaged into 5 s resolution to more easily compare with the HWB transformer data presented later in this study. The lower panel shows the Swampy Summit d*H*/d*t*, also with the 1 s data averaged into 5 s resolution.

Although there are many temporal similarities between the magnetic field changes at Eyrewell and Swampy Summit, it is clear that d*H*/dt measured at Swampy Summit is larger on several occasions. This is particularly noticeable for the events at 11:30 UT and 12:30 UT, both in the positive and negative rates of change where Eyrewell experienced just +20 to -20 nT/5s compared with +50 to -80 nT/5s at Swampy Summit. This suggests enhanced GIC currents likely to be flowing in the region local to Dunedin in these cases (Rodger et al., 2017). The event just before 09:00 UT is comparable in amplitude for both Eyrewell and Swampy Summit (-50 c.f. -70 nT/5s), suggesting a larger scale geomagnetic perturbation over a large fraction of the South Island. The symmetric spikes in the Swampy Summit data at 23:00UT are artifacts, and that period is not considered further in this study.

Since 2017 the nature and number of GIC-impacted transformers in the HWB substation have changed significantly. Initially there were two transformers at HWB earthed on the high voltage side (which makes them susceptible to GIC). The transformers were the single phase bank transformer T4, and a three phase, three limb autotransformer T6. In November 2017 T4 was decommissioned. In mid-2019 a new three phase transformer was added, identified as T3. Figure 2 shows the HWB substation single line diagram configuration during the Gannon storm in May 2024. Key high voltage transformers are T3, T5, and T6. All are 3 phase, 3 limb transformers. However, T5 is not earthed on the high voltage side and is therefore not susceptible to GIC.

Key points to note in Figure 2 are that T3 and T6 have DC measurements made through NCTD3 and NCTD6 respectively. These DC neutral current transformer measurements are made with LEM Hall-effect sensors, as described in Mac Manus et al. (2017). T3 (denoted by its vector group as YNd3) is a two-winding transformer, 220 kV to 33 kV. In the vector group uppercase letters refer to the high voltage winding and lowercase to the low voltage winding. T3 is a 3 phase, 3 limb transformer where the 220kV winding is in a star (wye) configuration and with the neutral earthed. T5 (Dyn3) has the 220 kV winding in a delta configuration and the 33 kV in star, earthed via a neutral earthing resistor (NER5) on the low-voltage side, i.e., 'n'. T6 (YNa0d9) is a 3 phase, 3 limb 220/110 kV wye configuration autotransformer with a common neutral-ground connection, i.e., 'N'. Power system modelling undertaken using PSCAD at the University of Canterbury High Voltage Laboratory indicates that the autotransformer T6 is more susceptible to GIC than the star-delta transformer T3, while T5 is hardly susceptible at all. Thus, in this study we concentrate our analysis on the DC measurements made for T6 and T3. Measurements of reactive power, *Q*, are provided for T6 through the power meter located at CB592, seen in the single line diagram just below T6. Reactive power, *Q*, measurements are provided for T3 through the power meter located at CB2412, seen in the single line diagram just below T3. Given the location of the meters described above the measurements may include Q from other transformers. However, as the lower voltage transformers within the substation are not affected by GICs, it is highly likely that a significant portion of the Q measurements assigned to each transformer as described above are due to that transformer. The units of *Q* are typically expressed as Volts-Amps-reactive (VAr) rather than power (W) to clearly identify that no work is done by the transformer, rather it is an absorption of power within the transformer. GIC-induced reactive power consumption is denoted in this study by Q_{con}. The units of *Q* and Q_{con} presented here are given in MVAr.

3 GIC and Harmonic distortion responses on 11 May 2024

The neutral current measured by the LEMs on T6, T3, and for the total current passing through the substation electrode, i.e., T6+T3, on 11 May 2024 are shown in Figure 3. The T3 and T6 data are provided by Transpower with 5 s resolution, while the total GIC is the signed sum of T3 and T6. In previous papers corrections for the return current induced by the operation of the high voltage DC (HVDC) link between South Island and North Island would have been removed (following the approach described in Mac Manus et al. (2017)). On 11 May the return current correction for HWB, due to HVDC operation, was typically <2 A after 13:00 UT, and 0 A before 13:00 UT. Those small currents have not been removed from the data shown, as the combination of HVDC offset and the storm induced GIC should both contribute to the generation of even harmonics during transformer saturation conditions. However, for simplicity, and because of the dominance of the GIC currents in this dataset, they will be identified as GIC levels. It should be noted that the measured GIC are the GIC from all three phases, so to determine the GIC in individual transformer windings the values would need to be divided by 3 to give GIC in A/phase. High GIC events occurred just before 09:00 UT, at 11:30 UT and 12:30 UT consistent with the times of high dH/dt shown in Figure 1. At these times the HVDC return current was 0 A, and no corrections for return current are needed. Typically, T6 experiences slightly higher GIC levels than T3, with a peak value of 113 A (c.f. 93 A) during the largest event at 12:30 UT. The total substation current passing through the substation earth electrode on 11 May 2024 is shown in the lower panel, showing several events exceeding 100 A, and a peak value of >200 A. Following the large current event at 12:30 UT lower levels are seen until the end of the day. In order to focus on the more disturbed period, subsequent analysis will be undertaken on the period 00:00 – 14:00 UT.

When distortion of the fundamental 50 Hz AC frequency occurs as a result of storm-induced GIC, even order harmonics occur due to half-cycle saturation, particularly those with lower orders, i.e., 2nd and 4th order harmonics. Clilverd et al. (2018) reported the observation of even order harmonics up to the 30th order, likely generated by a single bank transformer T4 in HWB during the 7-8 September 2017 geomagnetic storm. Although some individual harmonics were shown in Clilverd et al. (2018) the majority of the correlation analysis with GIC levels was undertaken using a 100 - 600 Hz average (i.e., including both even and odd order harmonics). In Figure 4 the variations of the average signal in the 100 - 600 Hz range, the ~100 Hz bin (2nd harmonic), and the ~200 Hz bin (4th harmonic) are shown for 00:00 – 14:00 UT, 11 May 2024. As in the magnetic field plot (Figure 1) and the HWB GIC plot (Figure 3), large events can be seen just before 09:00 UT, 11:30 UT, and at 12:30 UT in all three panels, a, b, and c. Several other smaller events can also be seen throughout the 00:00 – 14:00 UT disturbed period, consistent with smaller events seen in the GIC data shown in Figure 3.

The harmonics data plotted in the first 3 panels of Figure 4 are derived from an uncalibrated very low frequency magnetic loop antenna located very close to the HWB substation as described in Clilverd et al. (2018). It is important to note here that the signals recorded by the antenna will represent the whole substation output, and can not be attributed to any single transformer, unless there is clear evidence of a single dominant source inside the substation (as was the case in September 2017). In raw form the data are expressed in dB relative to the maximum possible sound card voltage, following an FFT performed with a frequency bin size of 23.4375 Hz (i.e., 48000/2048). Here the dB values are converted to linear values, and normalised to the median value of all samples at that frequency over the period 00-14:00 UT. This takes into account the background levels of the signals in each frequency bin. The normalised value of 1 is shown in each panel as a horizontal dotted line. Figure 4 (a) shows an average of the changing amplitude across all of the even and odd harmonics from 100 – 600 Hz inclusive, i.e., the 2nd to 12th harmonic. The normalised amplitude values are centered on a value of 1 as expected, and range up to a factor of 4 times enhancement factor in signal relative to the background conditions during the 12:30 UT GIC event. Panels (b) and (c) show the 100 Hz and 200 Hz FFT bins processed in a similar way to panel (a). In these panels the enhancement factors for the 12:30 UT GIC event are much larger than the 100 – 600 Hz average, due to the mix of even and odd harmonics in the average panel rather than the focus on only even harmonic 100 Hz and 200 Hz responses (panels b and c, respectively). Larger enhancements in harmonic amplitude are seen for the 4th order harmonic frequency bin compared with the 2nd order harmonic bin, although the timing of the significant enhancements are similar in both panels. Panel (d) shows the even order voltage total harmonic distortion (ETHD) of the fundamental AC frequency as a percentage, logged by Transpower at CB.2412. As shown in the single line diagram in Figure 2, CB.2412 is located close to the T3 transformer. The data resolution of the ETHD is 10 minutes, and shows broad peaks in distortion of up to ~0.6% co-incident with the more structured peaks evident in the three harmonic panels above it. These observations provide confidence that even order harmonic distortion events are well captured by the measurements available, and show the advantages of the higher time resolution of the VLF harmonic data.

In Figure 5 the variation of normalized harmonic amplitudes recorded by the VLF instrument as a function of absolute GIC level occurring in HWB, T6+T3 GIC, are plotted for six harmonic components, over the period 00:00 -14:00 UT, 11 May 2024. The lefthand panels show the 2nd, 4th and 6th order harmonics, i.e., panels (a), (b) and (c), while the righthand side shows the 3rd, 5th, and 7th order harmonics, i.e., panels (d), (e) and (f). As in Figure 4, the normalised value of 1 is shown in each panel as a horizontal dotted line. Clearly the even order harmonics on the lefthand side of the figure respond more to GIC level than the odd order harmonics on the right. All y-axis scales are set to a 0 - 25 range and confirm that the 4th harmonic (200 Hz) exhibits the largest responses in this frequency range. Similar harmonic amplitude responses occur for positive and negative polarity GIC. The 100 Hz and 200 Hz (2nd and 4th) harmonic panels show quasi-constant and low-level responses to GIC within 50 or 70 A, with enhancement factors typically <2. However, for GIC > 70 A the harmonics increase in amplitude steadily to exhibit peak values at the highest current levels observed during this time period. To a lesser extent this is also seen in several of the other frequency bins shown. The righthand panels in Figure 5 show the 3rd, 5th, and 7th odd order harmonics. Although, as expected, there are enhancements in the amplitude with increasing GIC level >~50 – 70 A, the responses are smaller than the even order harmonics, consistent with the bias of half-cycle asymmetric saturation towards even harmonic production.

We suggest the harmonic response shown in Figure 5 is caused by even order harmonic generation through asymmetric half-cycle transformer saturation when substation GIC levels exceed ~50 - 70 A (very roughly 25-35 A for each transformer). Transformers T6 and T3 are both three phase, three limb units, so these observations suggest that the threshold of susceptibility for such units is close to this level. At HWB the GIC is shared almost equally between T6 and T3 (as shown in Figure 3), with T6 expected to be more likely to experience saturation than T3, thus Figure 5 suggests that the generation of harmonics through saturation starts at about half the GIC level shown, i.e., ~25-35 A, and this should mostly be generated by T6. This conclusion is explored further in the reactive power section below.

4 Reactive power responses

During the Gannon storm period and particularly 00 – 14 UT on 11 May 2024, multiple occurrences of high GIC levels were measured at HWB and in the three phase, three limb transformer, T6 in particular. At the same time, enhanced even order harmonics were observed by the nearby VLF instrument, suggesting that asymmetric half-cycle saturation was occurring. Given high GIC levels, with resultant transformer saturation, a response in the T6 or T3 reactive power consumption, defined here as Q_{con}, would be expected. The relationship between Q_{con} and GIC level is an important factor in understanding high voltage transformer responses to extreme geomagnetic disturbances, and in the capability of the power grid to provide the necessary power to maintain the network stability in those circumstances.

In the following plots reactive power data is presented from power meter measurements made at the circuit breakers CB.592 (associated with T6), and CB.2412 (associated with T3). Both of which can be located in the single line diagram shown in Figure 2, where the circuit breakers are in series with labelled current transformers (CT) with the same number. Figure 6 shows the variation of GIC in T6 at HWB over a 1.3 hour period, starting at 11:18UT, ending at 12:36 UT, which encompasses the two largest events, i.e., at about 12:30 UT (largest) and also at about 11:30 UT (next largest) on 11 May 2024. Due to the symmetric response to the sign of the induced currents as seen in Figure 5, absolute GIC values are plotted in panel (a) with the blue line representing the GIC in T6, and the dotted red line representing T3. Both events exhibit a double peak structure with the largest GIC levels > 50 A in both transformers. As expected the time variation of the GIC in the two transformers is the same, except for relatively small differences in the magnitudes, most likely due to small differences in the resistance of the two transformers and their connections to earth. Figure 6 (b) shows the variation of the 4^{th} harmonic (200 Hz) over the same period. Enhancements of the 4^{th} harmonic above the baseline amplitude level determined by the median of the 00:00 – 14:00 UT period are shown (red line). The two events are clearly seen with double peak structures consistent with the GIC panel.

Figure 6 (c) and (d) show the consumption of reactive power, Q_{con}, measured from CB.592 (T6) and CB.2412 (T3) respectively. Both panels plot Q_{con}, relative to the median Q determined for each transformer over the period shown in the figure, i.e., in both cases the baseline Q was about -4 MVAr. The calculated median normalization baseline is indicated by a dot-dashed black line in both panels. In the T6 reactive power two events can be clearly seen with peak responses in Q_{con} at the times of increased GIC level in T6, and also with enhanced even order harmonic amplitude in the 200 Hz VLF channel. The T3 reactive power variation also shows a peak during the GIC event with the largest current, i.e., at about 12:30 UT, but less obvious GIC-driven peaks at other times. The largest event shown in Figure 6 has GIC ~100 A, 4^{th} harmonic enhancement of a factor of >25, and an increase in reactive power consumption of ~3 MVAr in T6, and <2 MVAr in T3, which is consistent with the suggestion that T6 is more responsive to GIC than T3.

One other time range stands out in the reactive power data from CB.592 during 11 May 2024, i.e., a half hour period around 09:00 UT. Figure 7 shows the T6 GIC, 4^{th} harmonic amplitude enhancement, and reactive power variations from CB.592 from 08:36 UT to 09:06 UT in the same format as Figure 6. Multiple intervals with > 30 A GIC in T6 are seen to produce 4^{th} harmonic amplitude enhancements, and increases in consumed reactive power in T6, but these are not seen in the reactive power data for T3. The largest event in this time period produced >70 A GIC, a 4^{th} harmonic amplitude enhancement of ~15, and an increase in Q_{con} of ~1.5 MVAr in T6.

In both Figure 6 and Figure 7, large GIC, even harmonic enhancements, and increased reactive power consumption occur for approximately 1-2 minutes at a time, with the longest sustained period lasting approximately 3 minutes. However, a sample resolution of 5 s for each dataset provides the opportunity to further investigate in more detail the relationships between the various parameters – as is undertaken below.

Figure 8 presents a three panel plot which shows (a) the summed GIC-induced variation of HWB reactive power ($Q_{con(T6+T3)}$) as a function of substation 4^{th} harmonic amplitude enhancement, (b) T6 reactive power consumption as a function of T6 GIC, and (c) T3 reactive power consumption as a function of T3 GIC levels. The data are taken from both periods shown in Figures 6 and 7, i.e., totaling 1.8 hours or 1296 data points. Each *Qcon* is given in terms of the difference from the background level over each period, determined by the median Q value. In every panel, the non-disturbed level of zero MVAr determined relative to the median is indicated by a black dot-dashed line. The red symbols represent the data from the period shown in Figure 6, while the black symbols represent the data from the period shown in Figure 7. Pearson correlation coefficients, R^2, and slope values are given for both event periods combined, i.e., the full 1.8 hours of data. The linear fit to the data in each panel is shown by a blue dotted line, with a starting point given by an enhancement factor of 2 in panel (a), as suggested by analysis of Figure 5, and ~30 A in panels (b) and (c) as suggested by Figure 5 and confirmed later in this paper. Correlation coefficients for the overall HWB response is high, as is the coefficient value for T6. However, for T3 the correlation coefficient is much lower, and then only found at this level by introducing a delay in the timing between GIC and Q_{con} of ~20 s, where Q_{con} lags GIC. This level of delay is not found in the T6 analysis, or the substation-wide generation of the 4th harmonic. In these cases the highest correlations are obtained with only 5 s delay, i.e., one data sample, between the driver and the reactive power response. However, previous work has shown reactive power delays of ~60 s for the time to saturation [Bolduc et al., 2000), and 95 s in analysis of Wye-Delta transformers (like T3) undertaken at the University of Canterbury High Voltage Laboratory (Subritzky et al., 2024). From all of the panels of Figure 8 it is clear that the two study periods (shown either by the red or black symbols) exhibit very similar behavior. For GIC <~30 A in T6 and T3, no obvious deviation from the background levels (determined from the median Q around the time of the event) can be seen.

The linear fit lines shown in Figure 8 have been identified through a process by which linear correlations are performed as a function of lower cutoff threshold of GIC value. Correlations are performed without using any of the data points below a varying GIC threshold to investigate the most-likely value. Figure 9 shows the result from varying the cutoff threshold for T6 GIC correlated against the CB.592 Q_{con} data (black line), and the T3 data correlated against the CB.2412 Q_{con} data (red line). For T6 the peak correlation value found was when the cutoff threshold was 30 A, and for T3 the peak was found at 28 A, indicated by black and red vertical dashed lines respectively. These levels are consistent with the Transpower SCADA alarm setting of ±25 A neutral DC current for their 3 phase, 3 limb transformers. For cutoff GIC values above these key thresholds R^2 slowly reduces as the number of pairs of data samples decreases. For T6 there are 155 GIC-Q_{con} data pairs above 30 A, suggesting that R^2=0.90 has very high significance, and a standard error of 0.02. For T3 there are 169 GIC-Q_{con} pairs above 28 A, similarly suggesting high significance even at a R^2 of 0.48, with a standard error of 0.06.

5 Discussion

Using a combination of measurements made in and around the Halfway Bush substation in Dunedin, South Island, New Zealand, it has been possible to trace the effects of the May

2024 Gannon geomagnetic storm on three phase, three limb transformers. Within the main storm period, multiple space weather-driven geomagnetic disturbance events, occurred each lasting 1-3 minutes. Such events were associated with large GIC in the substation, as well as external signs of even order harmonic amplitude enhancements caused by asymmetric half cycle saturation in individual transformer cores. The results shown in Figures 5, 9, and 10 suggest that above GIC levels of 28-30 A, the three phase, three limb transformers in the HWB substation began to show increased reactive power consumption. The reactive power consumption varies linearly with GIC level above this dc threshold and is consistent with the behaviour seen for enhanced even order harmonics associated with asymmetric half-cycle saturation (e.g., Rezaei-Zare et al., 2016).

When considering the reactive power response of the three-phase transformer, T6, to GIC level three important findings have been identified. Firstly, there appears to be a GIC threshold required before a reactive power response, which is at ~30 A. This is consistent with the findings identified using the even order harmonic VLF observations, which also determined a GIC threshold value of 25-35 A. This suggests that above 30 A reactive power begins to be absorbed within the three phase transformer, potentially driving increases in internal temperature. Above the threshold there is a linear relationship between GIC and reactive power consumption, exhibiting a high correlation coefficient. This holds for a range of GIC level from 30 to 113 A, and is found to be independent of the sign of the current. For transformer GIC levels >30 A the relationship between Q_{con} and induced current is 0.038MVAr/A. The threshold behaviour and linear reactive power gradient determined here is consistent with the transformer modelling study of Rezaei-Zare et al. (2016). However, the determined gradients for T6 and T3 are about a factor of 2-4 smaller than the Rezaei-Zare modelling, as shown in Figure 5 of that paper. This difference suggests that the HWB transformers are less reactive than expected from that modelling study, but with a neutral current threshold level within the range modelled in that study, i.e., a range of 25-100 A. However, it is possible that the Rezaei-Zare modelling is done for GIC per phase (although this is not clear from that study), which would account for the near factor of 3 difference between the modelling study and the results presented here. The gradients found in this study for 3 phase, 3 limb transformers (0.038 and 0.026 MVAr/A) are about a factor of 10 lower than determined by Dong et al. (2001), and a factor of 4 lower than Bonmann et al. (2024). However, Dong et al. analysis was based on a 300 MVA, 500/230 kV transformer and Bonmann et al. was for a 420 kV autotransformer, both of which operate at higher line voltage levels than the 220/110 kV (T6) and 220/33 kV (T3) transformers at HWB. These different system operating voltages, with their different transformer, grounding, and transmission line resistances, are expected to be a significant factor in determining GIC-transformer responses.

Lapthorn et al. (2023) presented the results of a DC injection campaign undertaken with the assistance of Transpower Ltd in New Zealand during January 2023. The inter-island HVDC link was used to inject DC into the ground at Haywards substation in Wellington. The three phase, three limb 216 MVA, 220/110 kV autotransformer T5 was monitored for even order harmonic distortion, and reactive power consumption. The configuration of T5 at Wellington is similar to T6 at HWB. Increases in even order harmonic amplitude were observed in T5 for injected current > 25 A – suggesting the onset of saturation at a level that is consistent with the findings in this study. However, Lapthorn et al. (2023) did not observe any clear variation in reactive power consumption at the time (Q_{con} probably < 0.5 MVAr), which would also be expected from the findings of this study as the reactive power consumption at that GIC level would be small and difficult to detect. The findings in Lapthorn et al. (2023) and this study for 220/110 kV 3 phase, 3 limb wye-grounded transformers in New Zealand are consistent in characterizing the onset headroom levels at which saturation occurs.

The neutral GIC threshold and gradient results identified in this study can be put into context through the extreme geomagnetic disturbance modelling results shown in Figure 5 of Mac Manus et al. (2022). In that study HWB T6 was modelled with >2000 A peak GIC, based on a 4000 nT/min event scenario (Hapgood et al., 2021). Assuming the slope remains linear to very high GIC, the worst-case compensation required for the T6 reactive power consumption response to this extreme disturbance GIC level is an additional 75 MW to be provided by the grid for this one transformer. However, the assumption of a linear slope to very high GIC levels is contrary to the 3 phase, 3 limb magnetizing curve modelling study of Dong et al. (2001), where lower response gradients would be expected for very large GIC.

Transpower New Zealand Ltd have a geomagnetic storm mitigation plan, as described in Mac Manus et al. (2023). Principally through removing targeted transmission lines, GIC in key transformers/substations are significantly reduced once the plan is enacted. For an extreme storm scenario Mac Manus et al. (2023) identified that there would be 19 substations which would be experiencing GIC >50 A averaged over an hour even after mitigation (see Figure 6 of that paper). Assuming all the high voltage side earthed transformers in the substations identified were three phase, and similar to T6, only the GIC above 30 A would result in reactive power consumption. Thus for the 19 sites shown there would be a total GIC current experienced by the network of ~7800 A after mitigation, and ~11600 A without. The total number of transformers earthed on the high voltage side in those 19 sites is 90, result in a reactive power demand of ~194 MVAr (i.e., 0.038 x (sumGIC-90 x 30)) = 194 MVAr) in the mitigation case, and ~338 A for non-mitigation. Additional reactive power demand would come from other units not listed in the Mac Manus study, but with GIC >30 A. As such the ~200-3500 MVar estimate for increased generation demand is likely to be a substantial underestimate and needs significantly more refined consideration in future work. In New Zealand generators are required to be able to produce 50% of their rated MW in capacitive MVAr while remaining at full output. Thus, a ~200-350 MVAr extra power draw is equivalent to the reactive power capacity of 3 - 6 of the turbines (out of 7) in the 850 MW Manapouri power station located on the South Island. It should be noted that this estimate is based on hourly average GIC levels, while the previous HWB paragraph was based on extreme 1-minute values.

6 Conclusions

The geomagnetic storm of 10-11 May 2024, which started at ~17:00 UT on 10 May 2024, generated large magnetic field perturbations in New Zealand for approximately 24 hours. As a result the national grid operator, Transpower New Zealand, enacted GIC mitigation plans in the first few hours of the storm, with stable network conditions only occurring from 00:00 UT on 11 May. This study focusses on the 11 May, 00:00 -14:00 UT period when geomagnetic activity was high, and the high voltage grid configuration in this region was stable. Analysis of GIC measurements made at two 3 phase, 3 limb transformers, T6 and T3, operating on the 220 kV bus in the Halfway Bush substation in Dunedin, South Island, showed neutral currents up to 113 A on their high voltage sides, with multiple short periods where GIC > 50 A for each transformer.

In this study GIC measurements made at the two transformers in the Halfway Bush substation in Dunedin (T6 and T3) were compared with VLF harmonic measurements made nearby by a radiowave receiver, and reactive power measurements, *Q*, made at key points in the substation. The data resolution was 5 s. The following conclusions were made:

- VLF measurements showed linear enhancements in even order harmonics, particularly for the 2nd and 4th harmonics, consistent with asymmetric half-cycle transformer core saturation when GIC levels were >25 – 35 A per transformer.

- Reactive power measurements, Q, made at T6 and T3 also showed increases when GIC levels were >30 A, consistent with the enhancement of even order AC harmonics and the indication of transformer core saturation.

- Above 30 A GIC per transformer reactive power consumption, Q_{con}, increased linearly as current increased with the 3 phase, 3 limb transformer T6 exhibiting a slope of 0.038 MVAr/A and transformer T3 a slope of 0.026 MVAr/A.

The Gannon Storm period studied here represents a large, but not extreme geomagnetic storm. However, multiple short lived periods of high GIC experienced by the Halfway Bush substation transformers have provided an insight into the saturation responses of the transformers, and their reactive power consumption as a result. Extrapolation of these findings to extreme storm modelling of the New Zealand high voltage grid with the line switching mitigation plan in place (Mac Manus et al., 2023) suggests that an additional ~200-350MVAr of generation would be required to compensate for increased reactive power consumption of 3 phase, 3 limb transformers during a Carrington-level event. Such additional power generation levels are likely to be within the capabilities of the generators to accommodate.

Acknowledgments

This research was supported by the New Zealand Ministry of Business, Innovation & Employment Endeavour Fund Research Programme Contract UOOX2002. The authors would like to thank Transpower New Zealand for supporting this study. We would also like to thank Wayne Cleaver of

Omexon New Zealand (previously Electrix Limited) for their assistance in facilitating the VLF measurements at Halfway Bush.

Open Research

Eyrewell magnetometer data availability including the 1-s data can be accessed via https://doi.org/10.21420/APJY-5050 . The Swampy Summit magnetometer data and the Halfway Bush VLF harmonic data for the 11 May 2024 can be found at: https://zenodo.org/records/14011808. The New Zealand LEM DC and reactive power data were provided to us by Transpower New Zealand with caveats and restrictions. This includes requirements of permission before all publications and presentations. In addition, we are unable to directly provide the New Zealand LEM DC data, derived GIC observations, or the reactive power data. Requests for access to the measurements need to be made to Transpower New Zealand. At this time the contact point is Michael Dalzell (Michael.Dalzell@transpower.co.nz). We are very grateful for the substantial data access they have provided, noting this can be a challenge in the Space Weather field (Hapgood & Knipp, 2016).

References

Arrillaga, J., & Watson, N. R. (2003). *Power system harmonics* (2nd ed.). Wiley.

Beggan, C. D., Beamish, D., Richards, A., Kelly, G. S. P., & Thomson, A. W. (2013). Prediction of extreme geomagnetically induced currents in the UK high-voltage network. Space Weather, 11, 407–419. https://doi.org/10.1002/swe.20065

Béland, J., & Small, K. (2004). Space weather effects on power transmission systems: The cases of Hydro-Québec and Transpower New Zealand Ltd. In I. A. Daglis (Ed.), Effects of space weather on technological infrastructure (pp. 287–299). Kluwer Academy.

Birkeland, K. (1908). Norwegian Aurora Polaris Expedition, 1902-3 Part 1. H. Aschehoug and Company, Christiania.

Bonmann, D., Carrander, C., Kleivi, R., Ohnstad, T., Bjorgvik, G., & Susa, D. (2024). On-site GIC withstand experiment on a 1000 MVA autotransformer and a 300 MVA 5-limb transformer Part 2: Measurements and Evaluation. International Council on large electrical systems (CIGRE), Paris Session, A2 Power transformers and Reactors, ID: 11033, 1-11.

Boteler, D. H., Shier, R. M., Watanabe, T., & Horita, R. E. (1989). Effects of geomagnetically induced currents in the BC Hydro 500 kV system. IEEE Transactions on Power Delivery, 4(1), 818–823. https://doi.org/10.1109/61.19275

Boteler, D. H. (2015). The Impact of Space Weather on the Electric Power Grid. In Heliophysics V. Space Weather and Society, by C. J. Schrijver, F. Bagenal, and Sojka. Palo Alto, CA: Lockheed Martin Solar & Astrophysics Laboratory

Bolduc, L., Gaudreau, A., & Dutil, A. (2000). Saturation time of transformers under dc excitation. Electric Power Systems Research, 56 (2), 95-102, https://doi.org/10.1016/S0378-7796(00)00087-0.

Clilverd, M. A., Rodger, C. J., Brundell, J. B., Dalzell, M., Martin, I., Mac Manus, D. H., et al. (2018). Long-lasting geomagnetically induced currents and harmonic distortion observed in New Zealand during the 7–8 September 2017 disturbed period. Space Weather, 16(6), 704–717. https://doi.org/10.1029/2018SW001822

Clilverd, M. A., Rodger, C. J., Brundell, J. B., Dalzell, M., Martin, I., Mac Manus, D. H., & Thomson, N. R. (2020). Geomagnetically induced currents and harmonic distortion: High time resolution case studies. Space Weather, 18(10), e2020SW002594. https://doi.org/10.1029/2020SW002594

Crack, M., Rodger, C. J., Clilverd, M. A., Mac Manus, D. H., Martin, I., Dalzell, M., et al. (2024). Even-order harmonic distortion observations during multiple geomagnetic disturbances: Investigation from New Zealand. Space Weather, 22, e2024SW003879. https://doi.org/10.1029/2024SW003879

Divett, T., Ingham, M., Beggan, C. D., Richardson, G. S., Rodger, C. J., Thom- son, A. W. P., & Dalzell, M. (2017). Modeling geoelectric fields and geomagnetically induced currents around

New Zealand to explore GIC in the South Island's electrical trans-mission network. Space Weather, 15(10), 1396–1412. https://doi.org/10.1002/2017SW001697

Divett, T., Mac Manus, D. H., Richardson, G. S., Beggan, C. D., Rodger, C. J., Ingham, M., et al. (2020). Geomagnetically induced current model validation from New Zealand's South Island. Space Weather, 18(8), e2020SW002494. https://doi.org/10.1029/2020SW002494

Dong, X., Liu, Y., & Kappenman, J. G. (2001). Comparative Analysis of Exciting Current Harmonics and Reactive Power Consumption from GIC Saturated Transformers. *2001 IEEE Power Engineering Society Winter Meeting. Conference Proceedings (Cat. No.01CH37194)*, 1, 318-322, https://ieeexplore.ieee.org/document/917055

Guillon, S., Toner, P., Gibson, L., & Boteler, D. (2016). A colorful blackout: The Havoc caused by auroral electrojet generated magnetic field variations in 1989. IEEE Power and Energy Magazine, 14(6), 59–71. https://doi.org/10.1109/mpe.2016.2591760

Hapgood, M., & Knipp, D. J. (2016). Data citation and availability: Striking a balance between the ideal and the practical. Space Weather, 14(11), 919–920. https://doi.org/10.1002/2016SW001553

Hapgood, M., Angling, M. J., Attrill, G., Bisi, M., Cannon, P. S., Dyer, C., et al. (2021). Development of space weather reasonable worst-case scenarios for the UK National Risk Assessment. Space Weather, 19(4), e2020SW002593. https://doi.org/10.1029/2020SW002593

Mac Manus, D. H., Rodger, C. J., Dalzell, M., Thomson, A. W. P., Clilverd, M. A., Petersen, T., et al. (2017). Long-term geomagnetically induced current observations in New Zealand: Earth return corrections and geomagnetic field driver. Space Weather, 15(8), 1020–1038. https://doi.org/10.1002/2017sw001635

Mac Manus, D. H., Rodger, C. J., Dalzell, M., Renton, A., Richardson, G. S., Petersen, T., & Clilverd, M. A. (2022). Geomagnetically induced current modeling in New Zealand: Extreme storm analysis using multiple disturbance scenarios and industry provided hazard magnitudes. Space Weather, 20(12), e2022SW003320. https://doi.org/10.1029/2022SW003320

Mac Manus, D. H., Rodger, C. J., Renton, A., Ronald, J., Harper, D., Taylor, C., et al. (2023). Geomagnetically induced current mitigation in New Zealand: Operational mitigation method development with industry input. Space Weather, 21(11), e2023SW003533. https://doi.org/10.1029/2023SW00353

Marshall, R. A., Dalzell, M., Waters, C. L., Goldthorpe, P., & Smith, E. A. (2012). Geomagnetically induced currents in the New Zealand power network. Space Weather, 10(8), S08003. https://doi.org/10.1029/2012SW000806

Oughton, E. J., Skelton, A., Horne, R. B., Thomson, A. W. P., & Gaunt, C. T. (2017). Quantifying the daily economic impact of extreme space weather due to failure in electricity transmission infrastructure. Space Weather, 15, doi:10.1002/2016SW001491

Price, P. R. (2002). Geomagnetically induced current effects on transformers. IEEE Transactions on Power Delivery, 17 (4), 1002 -1008, https://doi.org/10.1109/MPER.2002.4312311

Rajput, V., Boteler, D., Rana, N., Saiyed, M., Anjana, S., & Shah, M. (2020). Insight into impact of geomagnetically induced currents on power systems: Overview, challenges and mitigation. Electric Power Systems Research. 10.1016/j.epsr.2020.106927.

Rezaei-Zare, A., Marti, L., Narang A., & Yan, A. (2016). Analysis of three-phase transformer response due to GIC using an advanced duality-based model. *IEEE Transactions on Power Delivery*, 31 (5), 2342-2350, doi: 10.1109/TPWRD.2015.2505499

Rodger, C. J., Mac Manus, D. H., Dalzell, M., Thomson, A. W. P., Clarke, E., Petersen, T., et al. (2017). Long-term geomagnetically induced current observations from New Zealand: Peak current estimates for extreme geomagnetic storms. Space Weather, 15(11), 1447–1460. https://doi.org/10.1002/2017SW001691

Rodger, C. J., Clilverd, M. A., Mac Manus, D. H., Martin, I., Dalzell, M., Brundell, J. B., et al. (2020). Geomagnetically induced currents and harmonic distortion: Storm-time observations from New Zealand. Space Weather, 18(3), e2019SW002387. https://doi.org/10.1029/2019SW002387

Samuelsson, O. (2013). Geomagnetic disturbances and their impact on power systems. Industrial Electrical Engineering and Automation, Lund University.

Smith, A. W., Rodger, C. J., Mac Manus, D. H., Rae, I. J., Fogg, A. R., Forsyth, C., et al. (2024). Sudden commencements and geomagnetically induced currents in New Zealand: Correlations and dependance. Space Weather, 22, e2023SW003731. https://doi.org/10.1029/2023SW003731

Soren Subritzky, S., Lapthorn, A., Hardie, S., & Dalzell, M. (2024). DC Injection Testing of Power Transformers for Replicating GIC. International Council on large electrical systems (CIGRE), Paris Session, A2 Power transformers and Reactors, ID: 11843.

Transpower. (2024). Gannon geomagnetic storm: Event response summary and lessons learnt, Version 1.0, September 2024. https://static.transpower.co.nz/public/bulk-upload/documents/Event%204457%20-%20Gannon%20geomagnetic%20storm%20response%20summary%20and%20lessons%20learnt.pdf?VersionId=me4cehwLgGVV3f7V2ha0JafZhmikj1om

Vasseur, G., & Weidelt, P. (1977). Bimodal electromagnetic induction in non-uniform thin sheets with an application to the northern Pyrenean induction anomaly. Geophysical Journal International, 51(3), 669–690. https://doi.org/10.1111/j.1365-246X.1977.tb04213.x

Figures:

Figure 1: (a) The rate of change of the horizontal magnetic field component, H, at Eyrewell near Christchurch on 11 May 2024. (b) The rate of change of the magnetic field component, H, at Swampy Summit near Dunedin on 11 May 2024.

Figure 2: The 220 kV/110 kV high voltage section of the Halfway Bush substation single line diagram, representing the substation configuration during the May 2024 Gannon storm.

Figure 3: Variations of DC measured in the neutral-ground connection of HWB transformers on 11 May 2024. (a) T6. (b) T3. (c) The substation total electrode current. Note that the currents plotted are dominated by GIC, as described in the text.

Figure 4: The normalised amplitude variation of harmonics observed by the VLF instrument at HWB during 00:00 – 14:00 UT, 11 May 2024. The dashed line in all VLF amplitude panels corresponds to a value of 1.0. (a) The average 100 – 600 Hz signal. (b) 100 Hz bin (2^{nd} order harmonic). (c) 200 Hz bin (4^{th} order harmonic). (d) The percentage of even order total harmonic distortion (ETHD) from CB.2412, averaged over the 3 phases. Peaks in signal intensity occur at times consistent with large GIC shown in earlier figures.

Figure 5: The variation of normalized harmonic amplitudes as a function of absolute GIC level occurring in the HWB substation transformers, T6 and T3, for plotted for harmonic component of 2^{nd}, 3^{rd}, 4^{th}, 5^{th}, 6^{th}, and 7^{th} order (100 Hz – 350 Hz), over the period 00:00 -14:00 UT, 11 May 2024.

Figure 6: Measurements made at the HWB substation over a 1.3 hour period which encompasses the two largest events on 11 May 2024 at ~11:30 UT and ~12:30 UT (a) The variation of absolute GIC in T6 at HWB (blue line). (b) The variation of the 4th harmonic (200 Hz) above the baseline amplitude level (red line). (c) The variation of the reactive power (Qcon) for T6 from CB.592. (d) The variation of the reactive power (Qcon) for T3 from CB.2412.

Figure 7: Same format as Figure 6, but in this case for a half an hour period around 09:00 UT on 11 May 2024 (08:36 to 09:06 UT).

Figure 8: (a) The variation of combined T6 and T3 GIC-induced reactive power consumption, Qcon(T3+T6), as a function of substation 4th harmonic amplitude enhancement. (b) T6 reactive

power consumption as a function of T6 GIC. (c) T3 reactive power consumption as a function of T3 GIC levels. The data are taken from both of the active periods shown in Figures 6 and 7, i.e., totaling 1.8 hours or 1296 data points. Qcon is given in terms of the difference from the background level over each period, determined by the median Q value.

Figure 9: Linear Pearson correlation coefficients between reactive power variations with GIC level as a function of lower cutoff threshold of GIC level. T6 GIC correlated against the CB.592 Qcon data are shown by the black line, and the T3 data correlated against the CB.2412 Qcon data are shown by the red line (see Figure 2 for the single line diagram of the HWB substation). Vertical dotted lines indicate the threshold current value for highest R^2.

Figure 1.

(a)

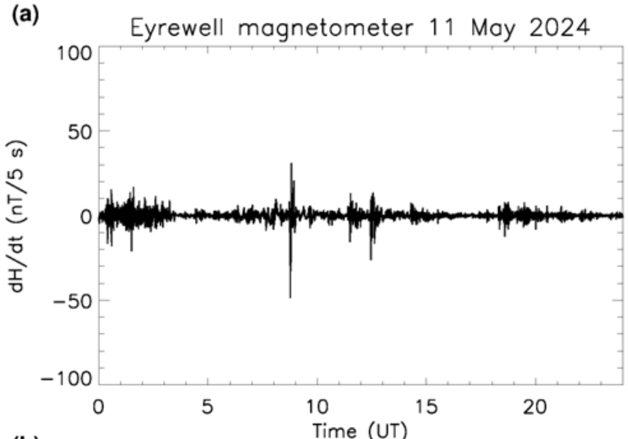
Eyrewell magnetometer 11 May 2024
100
50
0
−50
−100
dH/dt (nT/5 s)
0
5
10
15
20
Time (UT)

(b)

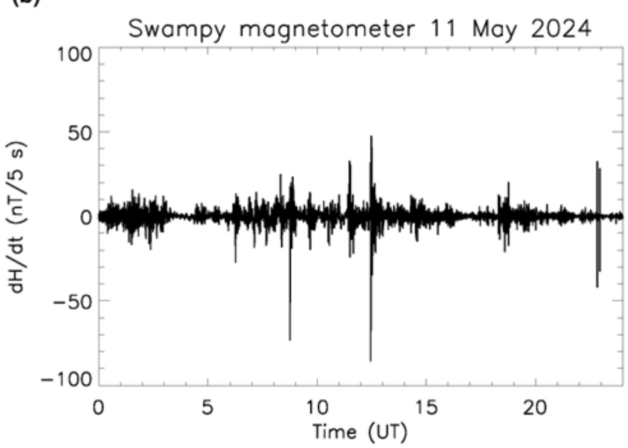
Swampy magnetometer 11 May 2024
100
50
0
−50
−100
dH/dt (nT/5 s)
0
5
10
15
20
Time (UT)

Figure 2.

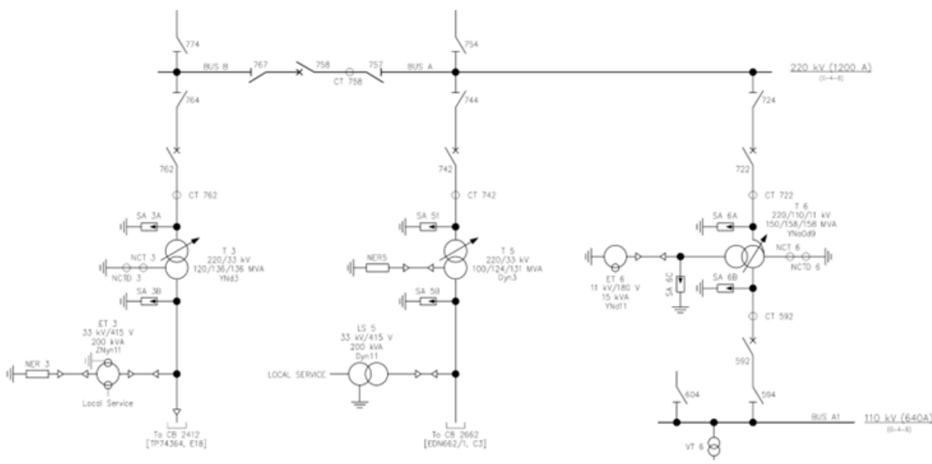

774
BUS B
767
758
CT 758
757
BUS A
754
220 kV (1200 A)
764
744
724
762
742
722
CT 762
CT 742
CT 722
SA 3A
SA 51
SA 6A
T 3
220/33 kV
120/136/136 MVA
YNd3
NCT 3
NCTD 3
SA 3B
T 5
220/33 kV
100/124/131 MVA
Dyn3
NER5
SA 58
T 6
220/110/11 kV
150/158/158 MVA
YNa0d9
NCT 6
NCTD 6
SA 6B
SA 6C
ET 6
11 kV/180 V
15 kVA
YNd11
CT 592
592
ET 3
33 kV/415 V
200 kVA
ZNyn11
NER 3
Local Service
LS 5
33 kV/415 V
200 kVA
Dyn11
LOCAL SERVICE
To CB 2412
[TP74364, E18]
To CB 2662
[EDN662/1, C3]
604
594
BUS A1
110 kV (640A)
VT 6

Figure 3.

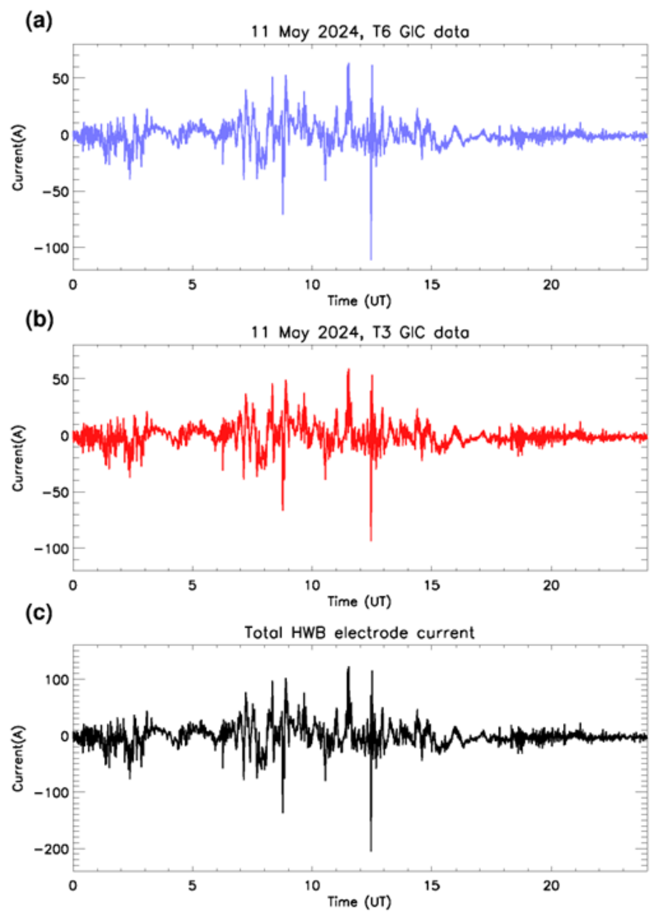
(a)
11 May 2024, T6 GIC data
Current(A)
Time (UT)
(b)
11 May 2024, T3 GIC data
Current(A)
Time (UT)
(c)
Total HWB electrode current
Current(A)
Time (UT)

Figure 4.

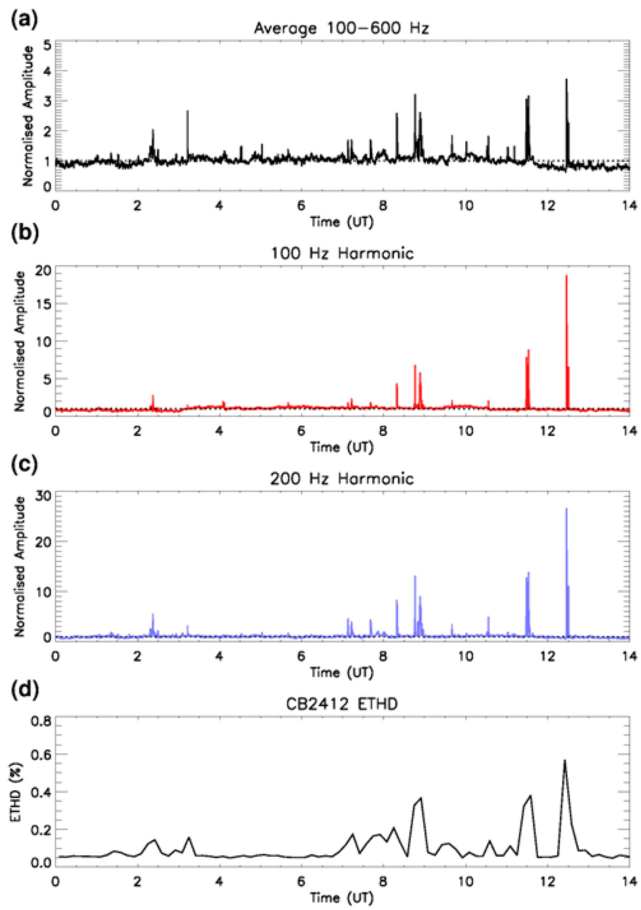

(a)
Average 100–600 Hz
Normalised Amplitude
Time (UT)
(b)
100 Hz Harmonic
Normalised Amplitude
Time (UT)
(c)
200 Hz Harmonic
Normalised Amplitude
Time (UT)
(d)
CB2412 ETHD
ETHD (%)
Time (UT)

Figure 5.

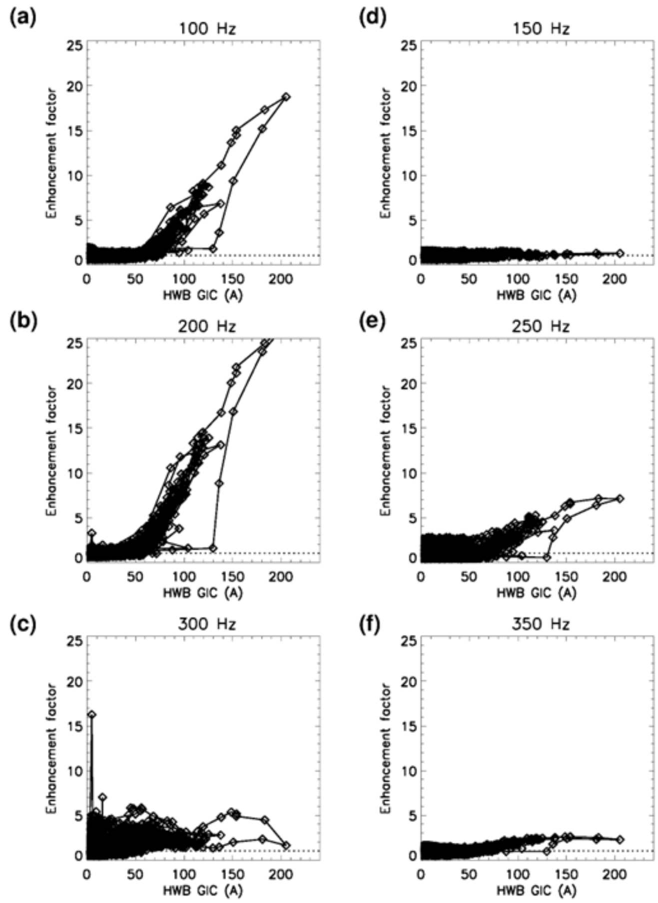
(a)
100 Hz
(b)
200 Hz
(c)
300 Hz
(d)
150 Hz
(e)
250 Hz
(f)
350 Hz
Enhancement factor
HWB GIC (A)

Figure 6.

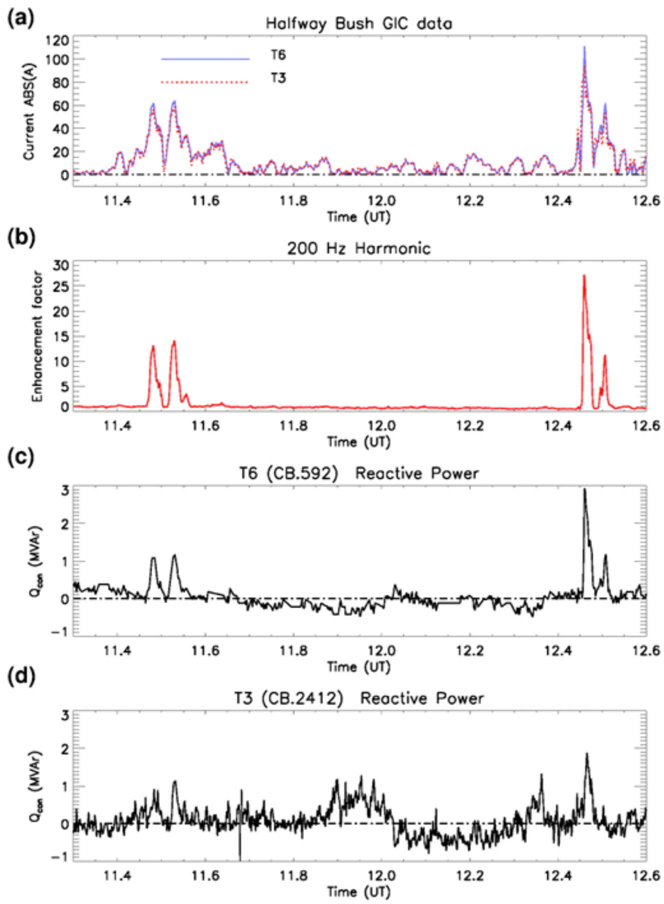
(a)
Halfway Bush GIC data
T6
T3
Current ABS(A)
Time (UT)
(b)
200 Hz Harmonic
Enhancement factor
Time (UT)
(c)
T6 (CB.592) Reactive Power
Q_{con} (MVAr)
Time (UT)
(d)
T3 (CB.2412) Reactive Power
Q_{con} (MVAr)
Time (UT)

Figure 7.

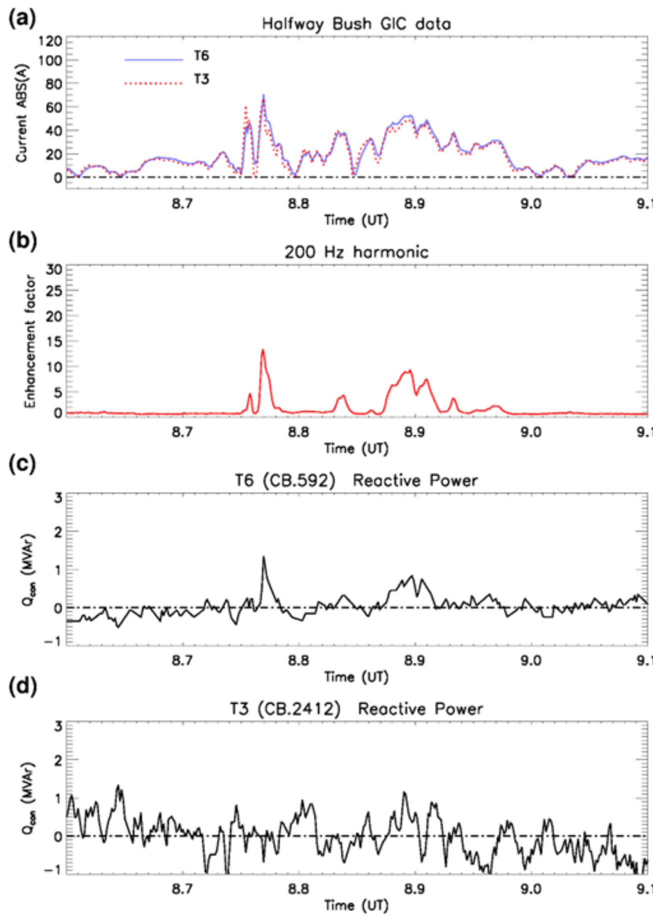
(a)
Halfway Bush GIC data
Current ABS(A)
120
100
80
60
40
20
0
T6
T3
8.7
8.8
8.9
9.0
9.1
Time (UT)
(b)
200 Hz harmonic
Enhancement factor
30
25
20
15
10
5
0
8.7
8.8
8.9
9.0
9.1
Time (UT)
(c)
T6 (CB.592) Reactive Power
Q_con (MVAr)
3
2
1
0
−1
8.7
8.8
8.9
9.0
9.1
Time (UT)
(d)
T3 (CB.2412) Reactive Power
Q_con (MVAr)
3
2
1
0
−1
8.7
8.8
8.9
9.0
9.1
Time (UT)

Figure 8.

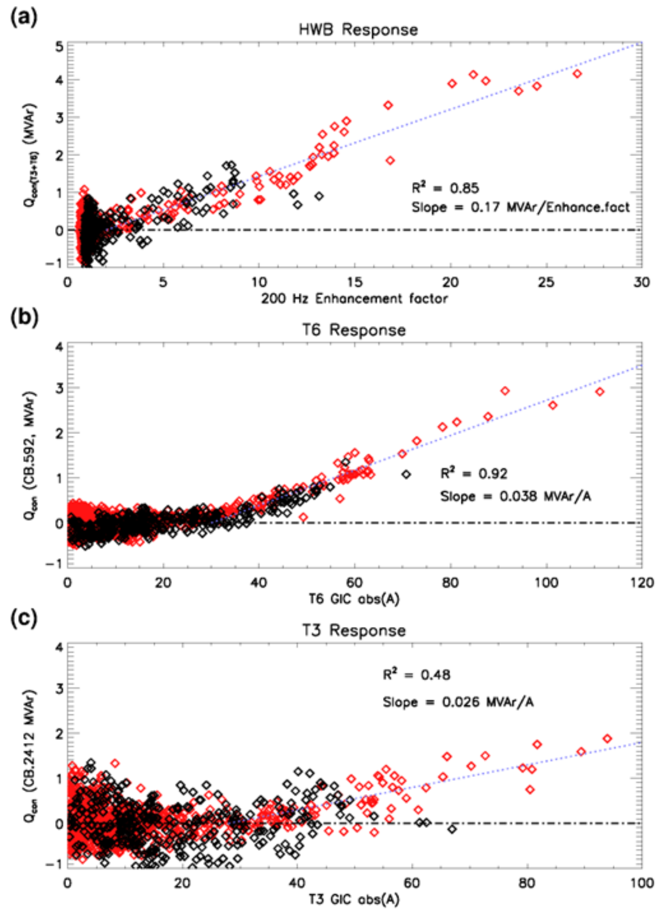
(a)
HWB Response
Q_con(T3+T6) (MVAr)
R² = 0.85
Slope = 0.17 MVAr/Enhance.fact
200 Hz Enhancement factor
(b)
T6 Response
Q_con (CB.592, MVAr)
R² = 0.92
Slope = 0.038 MVAr/A
T6 GIC abs(A)
(c)
T3 Response
Q_con (CB.2412 MVAr)
R² = 0.48
Slope = 0.026 MVAr/A
T3 GIC abs(A)

Figure 9.

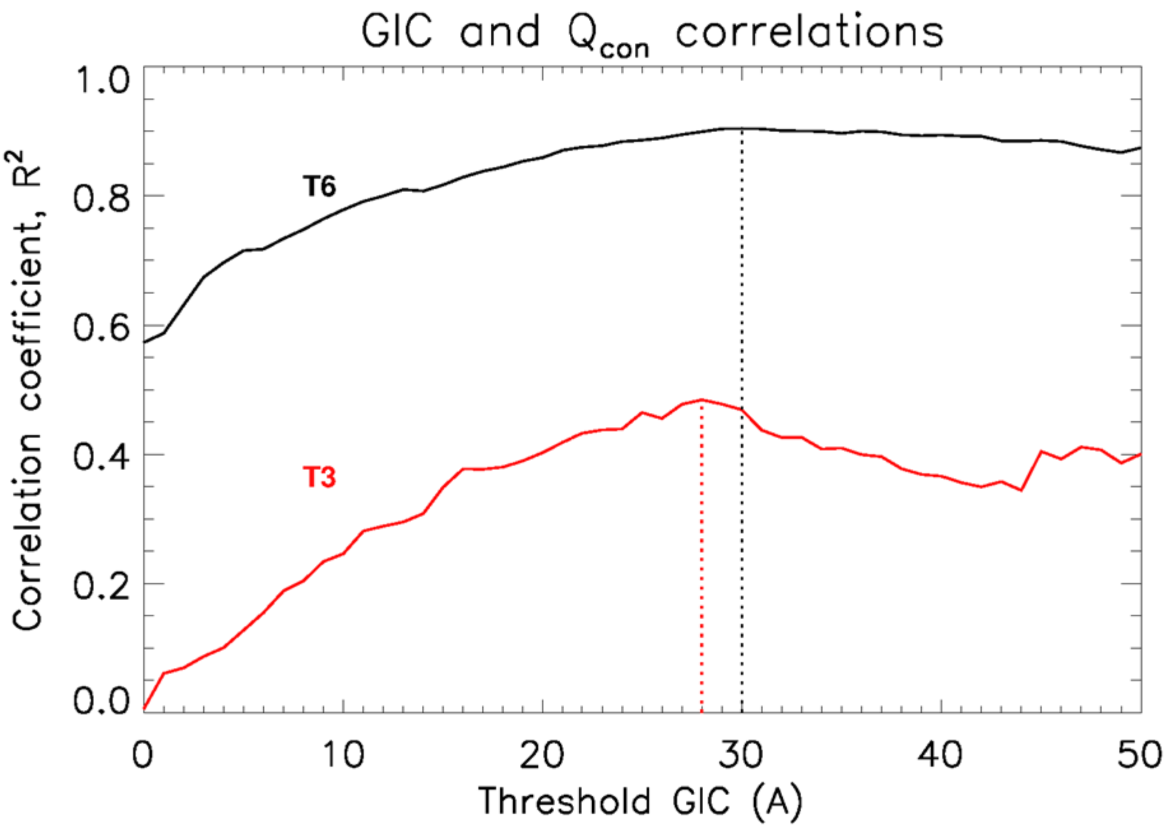

GIC and Q_{con} correlations
Correlation coefficient, R^2
Threshold GIC (A)
T6
T3
0.0
0.2
0.4
0.6
0.8
1.0
0
10
20
30
40
50